

Imaging the Reaction Dynamics of OH + CD₄. 3. Isotope Effects

Bailin Zhang,[†] Weicheng Shiu,[†] and Kopin Liu^{*,†,‡}

Institute of Atomic and Molecular Sciences (IAMS), Academia Sinica, P.O. Box 23–166, Taipei, Taiwan 10617, and Department of Chemistry, National Taiwan University, Taipei, Taiwan 10617

Received: July 5, 2005; In Final Form: August 7, 2005

Isotope effects in the reaction of hydroxyl radical with methane are investigated in a crossed-beam experiment. By exploiting different combinations of OH/OD + CH₄/CD₄/CHD₃, a total of eight isotopically variant reactions are examined to decipher the dynamical consequence of both primary and secondary isotope effects. The most prominent observation is from isotopic substitution of the transferred atom (primary isotope effect), which yields more stretch-excited water product for the D atom case than H atom. The opposite is found, however, for excitations in bending and combination modes. The secondary isotope effects, from either substituted hydroxyl radical or the three H atoms that are not being abstracted, are relatively minor and manifest themselves in spreading the vibrational distribution of the water coproducts.

I. Introduction

The kinetic isotope effect has long been recognized as a powerful means to unravel the detailed reaction mechanism and to provide further insights into the bond breaking and forming events in a chemical process.¹ A primary kinetic isotope effect is observed when the rate-determining step invokes the scission of a bond involving the isotope. A secondary kinetic isotope effect refers to the change in reaction rate even though the bond involving the isotope is not broken to form product. Because of the large disparity in mass when a H atom is substituted by a D atom, the kinetic isotope effect is usually most profound or most readily detected for a process involving hydrogen atom transfer.

In the reaction of OH + CH₄ → CH₃ + H₂O, both reagents contain hydrogen atoms. It is thus an interesting case to examine various isotope effects by substituting one or several D atoms for the five H atoms in the system. For example, if the substituted D atom happens to be the atom transferred from methane to hydroxyl in reaction, one has the primary isotope effect. On the other hand, if the substituted D atom does not actively participate in the old bond rupture and new bond formation, i.e., it is either as OD reagent or constitutes part of the “unreactive” methyl moiety throughout the reaction, the secondary isotope effects will be encountered. In addition to being a test bed for fundamental understandings of kinetic isotopic effect, the OH + CH₄ reaction is of great atmospheric importance.^{2,3} In particular, the use of isotopic variants of this reaction has been suggested to provide a potentially more informative clue as to the various sources of CH₄ in atmosphere, which is a long-standing issue in atmospheric modeling.⁴

Over the past decades, there have been numerous studies on isotope effects of this reaction, aiming for more accurate database for this purpose.^{5–12} One of the most recent experimental attempts is that by Gierczak et al.,¹² in which a critical comparison with previous measurements was made and the atmospheric implications of the new set of kinetic isotope data were also briefly discussed. Masgrau et al. subsequently reported

theoretical studies,¹³ using variational transition-state theory plus multidimensional tunneling corrections at high level ab initio electronic structure calculations, to understand the experimental isotope effects. Although the comparisons are reasonable, the computed results do not match exactly the available experimental data. Using the experimental rate constants and kinetic isotope effects as calibration criteria, Espinosa-Garcia and Corchado reported the first analytical potential energy for the OH + CH₄ reaction,¹⁴ for which dynamical features, such as reaction-path curvature and coupling between the reaction coordinate and vibrational modes, were analyzed.

In the preceding paper,¹⁵ we presented the translational energy dependencies of various dynamical attributes of the two product pairs for an isotopically variant reaction OH + CD₄ → HOD + CD₃. Reported here is an analogous study, but focusing on the isotope effects. More specifically, we exploited various combinations of OH/OD + CH₄/CD₄/CHD₃ reactions for this investigation. (Analogous reactions with CH₃D and CH₂D₂ are yet to be studied, due to the short of isotopic samples at the present time.) This results in eight isotopic variants, which enable us to take a closer look at the dynamic effects from both primary and secondary isotope substitutions.

II. Results and Discussion

(A) Raw Images and Product Speed Distributions. The experimental approach and procedures are the same as the preceding papers,^{15,16} and thus they will not be repeated here. Figure 1 exemplifies one image for each of the reactions in this study. The vibrational ground state of methyl radicals, which is the dominant product state, was probed for all images. For clarity, the corresponding reaction is listed at the bottom according to the labeled image. The collisional energy and Newton diagram are indicated with the image. All images feature several closely spaced, backscattered rings. (The beam-generated and vacuum backgrounds are readily identified from their appearances and verified experimentally.) Nonetheless, a closer inspection reveals the distinctions, and each image exhibits characteristic features different from others.

After the density-to-flux corrections to raw images,¹⁷ the resultant methyl radical product speed distribution, $P(\mu)$, for

* Corresponding author. E-mail: kpliu@gate.sinica.edu.tw.

[†] Academia Sinica.

[‡] National Taiwan University.

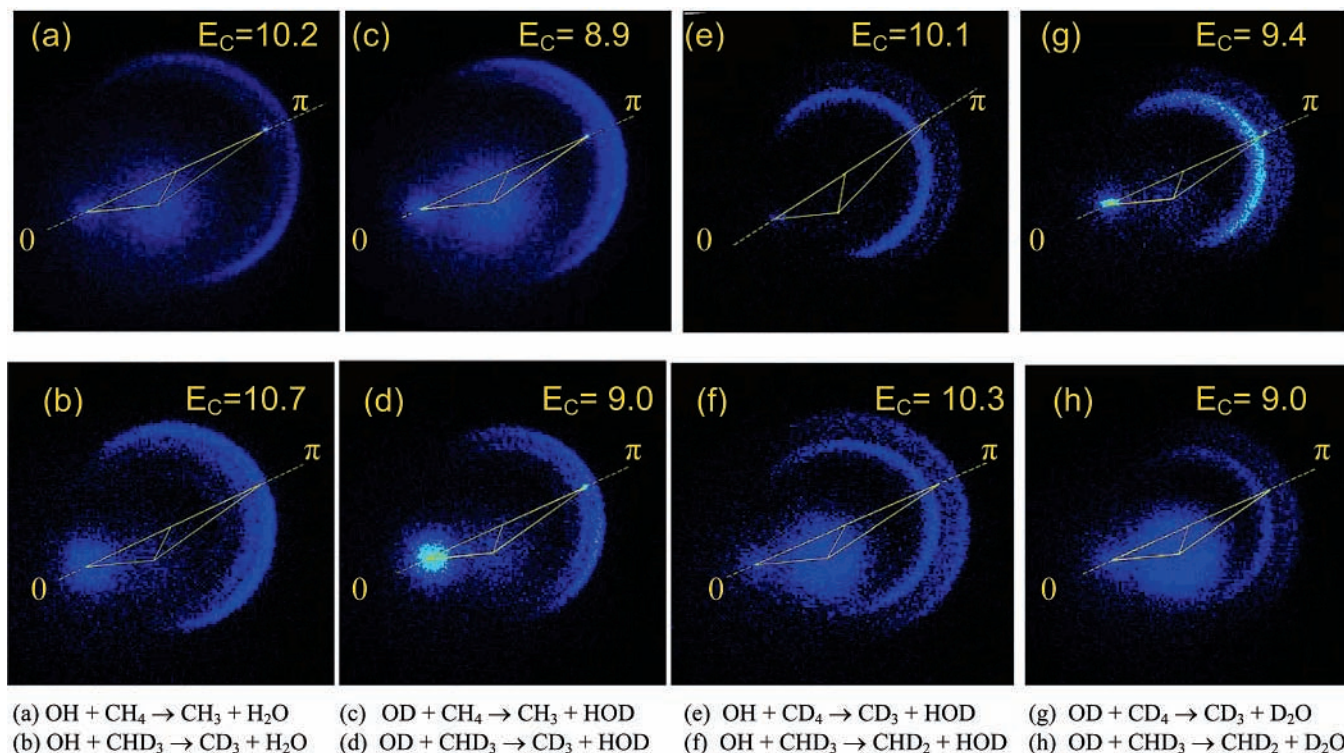


Figure 1. Eight representative raw images: one for each isotopic variant of reactions. The corresponding reactions are listed at the bottom, and are arranged in an order for ready comparisons.

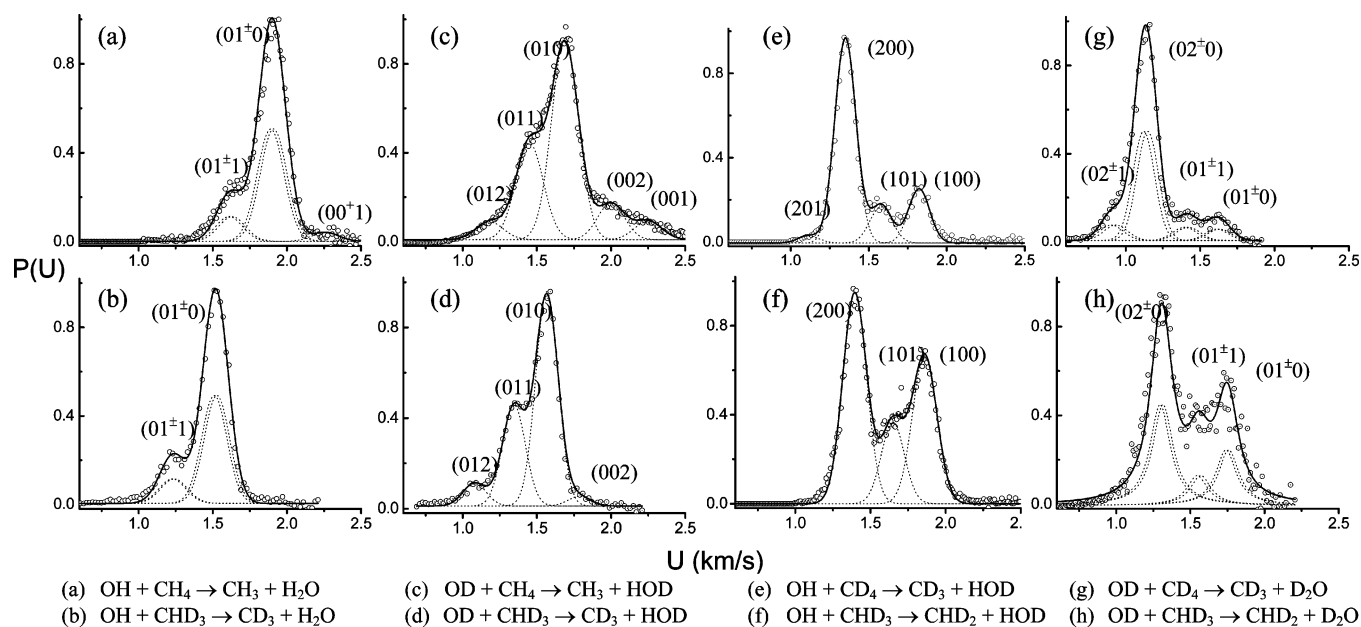


Figure 2. Methyl radical product speed distribution, $P(u)$, derived from the raw image shown in Figure 1. For convenience, the corresponding isotope reactions are also listed here. The coincidentally excited vibrational levels of the water coproducts are assigned on energetic grounds. (See text for the notation.) The dotted lines indicate their contributions and the solid line is the overall fit to the $P(u)$ distribution.

each of the images in Figure 1 is presented in Figure 2. As detailed in the preceding papers,^{15,16} the energetic of the systems are well-established. By conservations of energy and momentum, the peak structures of the $P(u)$ distributions were assigned accordingly as the vibrational levels of the water coproducts. (Hereafter, the term “water” product means the reaction product of H_2O , D_2O , or HOD .) As found in previous studies of $\text{OH} + \text{CD}_4$ ^{15,16} and $\text{OH} + \text{D}_2$,^{18–20} the vibrational excitation of the HOD product is mostly localized in the newly born OD oscillator, not in the old OH bond. For convenience of further

discussion, we therefore designate the vibrational level assignment as follows: $(\nu_{\text{OD}}\nu_{\text{OH}}\nu_{\text{bend}})$ for the HOD product, and $(n, m^\pm \nu_{\text{bend}})$ for H_2O and D_2O products in the local mode representation.²¹ Local-mode states of H_2O and D_2O are not the eigenstates. As a result of interbond couplings in Hamiltonian, the eigenstates are symmetry-adapted combination of (n, m) and (m, n) bond oscillators. The two nearly degenerate states are beyond our experimental resolution, we assumed an equal population when simulating the measured $P(u)$ distribution. The resultant overall fit is shown as the solid line, and the

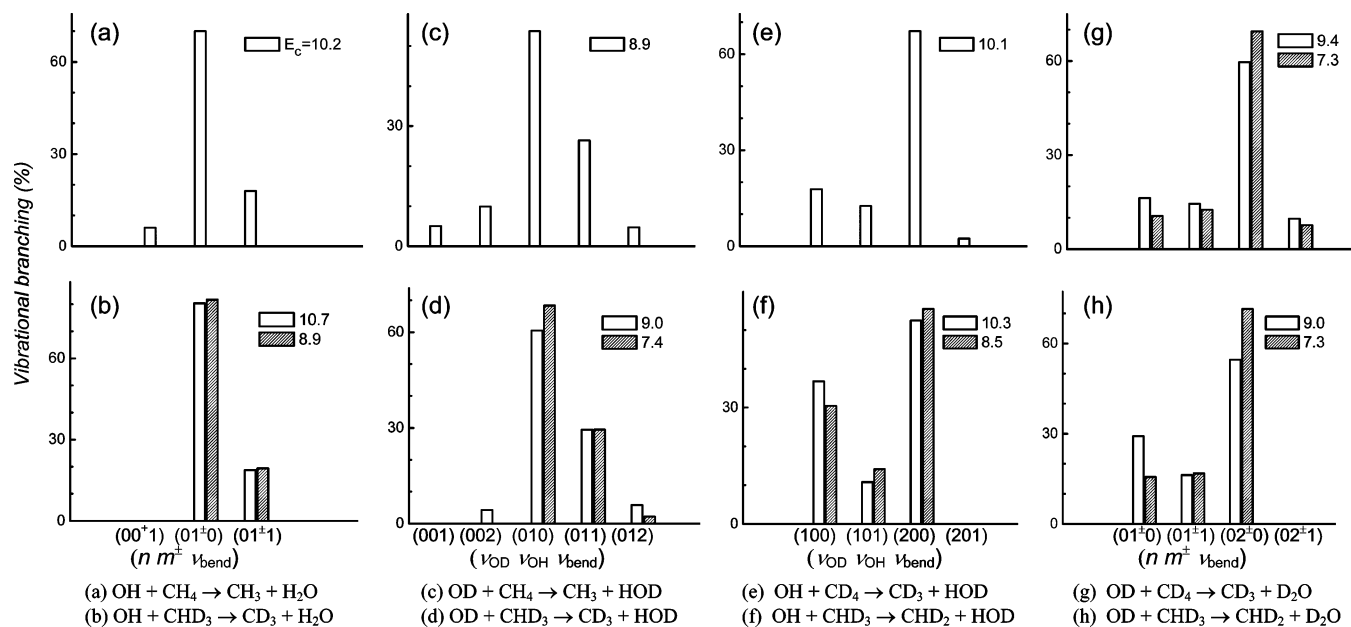


Figure 3. Summary of the correlated vibration branching of the water coproduct. The notation of the vibrational level and the isotope reaction are given at the bottom. Note the high specificity in vibrational distributions.

TABLE 1: Energy Disposal of Isotopic Variants of the OH + CH₄ Reaction

| reacn | $-\Delta H_0^a$ | ΔE_c^a | V^a | R^a | T^a | P_s^b | P_c^b | P_b^b | f_s | f_c | f_b |
|-------|-----------------|----------------|-------|-------|-------|---------|---------|---------|-------|-------|-------|
| a | 14.31 | 10.2 | 11.4 | 1.5 | 11.7 | 0.71 | 0.24 | 0.04 | 0.31 | 0.15 | 0.01 |
| b | 13.72 | 10.7 | 11.4 | 1.9 | 11.1 | 0.81 | 0.19 | 0 | 0.35 | 0.12 | 0 |
| | | | 8.9 | 11.5 | 1.8 | 9.3 | 0.80 | 0.20 | 0 | 0.38 | 0.13 |
| c | 14.61 | 8.9 | 10.7 | 3.7 | 9.2 | 0.54 | 0.31 | 0.15 | 0.24 | 0.2 | 0.04 |
| d | 14.02 | 9.0 | 12.0 | 2.0 | 8.9 | 0.61 | 0.35 | 0.04 | 0.30 | 0.24 | 0.01 |
| | | | 7.4 | 11.8 | 2.8 | 6.7 | 0.64 | 0.36 | 0 | 0.32 | 0.25 |
| e | 13.73 | 10.1 | 13.9 | 0.9 | 9.1 | 0.85 | 0.15 | 0 | 0.50 | 0.08 | 0 |
| f | 14.02 | 10.3 | 12.5 | 1.7 | 10.2 | 0.89 | 0.11 | 0 | 0.48 | 0.06 | 0 |
| | | | 8.5 | 12.8 | 0.9 | 8.8 | 0.86 | 0.14 | 0 | 0.49 | 0.07 |
| g | 14.15 | 9.4 | 12.7 | 3.1 | 7.8 | 0.76 | 0.24 | 0 | 0.49 | 0.13 | 0 |
| | | | 7.4 | 14.2 | 1.4 | 5.8 | 0.80 | 0.20 | 0 | 0.50 | 0.13 |
| h | 14.44 | 9.0 | 12.5 | 1.8 | 9.2 | 0.84 | 0.16 | 0 | 0.50 | 0.07 | 0 |
| | | | 7.4 | 13.9 | 1.7 | 6.3 | 0.88 | 0.12 | 0 | 0.51 | 0.08 |

^a In kcal/mol; the exothermicities are estimated from zero-point-energy differences, based on the value for reaction a. ^b P_s , P_c , and P_b refer to the probabilities for vibrational excitation of water products in different types of motions: stretch, combination mode, and bend, respectively. Similarly, f_i represents the fractional energy disposal into the i th type of water vibrations.

contribution from the individual, coincidentally formed state of the coproduct is depicted as the dotted line. Because the structural features are not completely resolved, the simulated results will not be unique. Nevertheless, the well-defined energetic and the goodness of fitting put considerable constraints on the level assignments. We believe that the slight uncertainty in fitting will not impact the conclusion of this study.

(B) Correlated Vibration Branching and Energy Disposal.

Figure 3 summarizes the vibrational branching of coproducts thus derived. Eight isotopically variant reactions are arranged in the same order as Figures 1 and 2, and for ready reference are indicated at the bottom of the figure. For convenience of discussion, some of the key results from data analysis are also presented in Table 1. In addition to the heat of reaction (ΔH_0) and collisional energy, the energy disposal into the vibration (V) and rotation (R) of water coproducts, as well as the correlated kinetic energy release (T) are summarized. We further highlight the excitation probability of the vibrational motions of water product in three categories: pure stretch (P_s), stretch-bend combination (P_c), and bending mode (P_b). Because of the

significant disparity in energies of three different types of vibrational motions, the fractional energy disposals, i.e., f_s , f_c , and f_b , are computed and tabulated.

Reactions a–d all invoke the H atom transfer from methane to the attacking hydroxyl radical, whereas reactions e–h are of the D atom transfer. The primary isotope effect is readily apparent from the gross patterns of the two classes of isotopic reactions. For the H atom transfer process, cases a–d, the product H₂O or HOD are stretch-excited, with almost exclusively one-quantum excitation in the newly born OH bond. While the products are also mainly stretch-excited for the D atom transfer reactions, cases e–h, the most populated state is now with two-quantum excitation in the new OD bond, and with a significant one-quantum excitation. Together, the D atom transfer reactions generally yield more stretch-excited products than the H atom transfer ones. This can be seen by comparing the vibrational branching of pure stretch-excitation for a pair of analogous reactions, e.g., cases a and e, b and f, c and g, and d and h, from Figure 3 or from the tabulated P_s values in Table 1. Alternatively, the same conclusion can be reached by noting that the fractional energy release into pure stretch for the H atom transfer reaction, f_s that clusters around 0.31 ± 0.07 , is significantly smaller than the value of $f_s \approx 0.5$ for the D atom transfer cases. Less stretching excitation for the former is partially compensated by more populations in the combination and/or bending modes than for the latter. Again, this can be appreciated by comparing either P_c (P_b) or f_c (f_b), as listed in Table 1, for the appropriate pair of reactions.

Two kinds of secondary isotope effects are possible: deuterium-substitution for the attacking OH radical or for the three H atoms that are not being abstracted from the target methane molecule. It is noteworthy that there will be little isotope effect if the hydroxyl radical really behaves as a spectator, as commonly assumed in the theoretical dynamics studies.^{22–25} Kinetically, it was found that this type of secondary isotope effect is indeed small, which can be comprehended from the small changes in the transition state for substituted and nonsubstituted systems in the context of transition-state theory.^{5–12} We begin below with the dynamic consequence for this kind of isotopic substitution when reacting with an identical methane reagent.

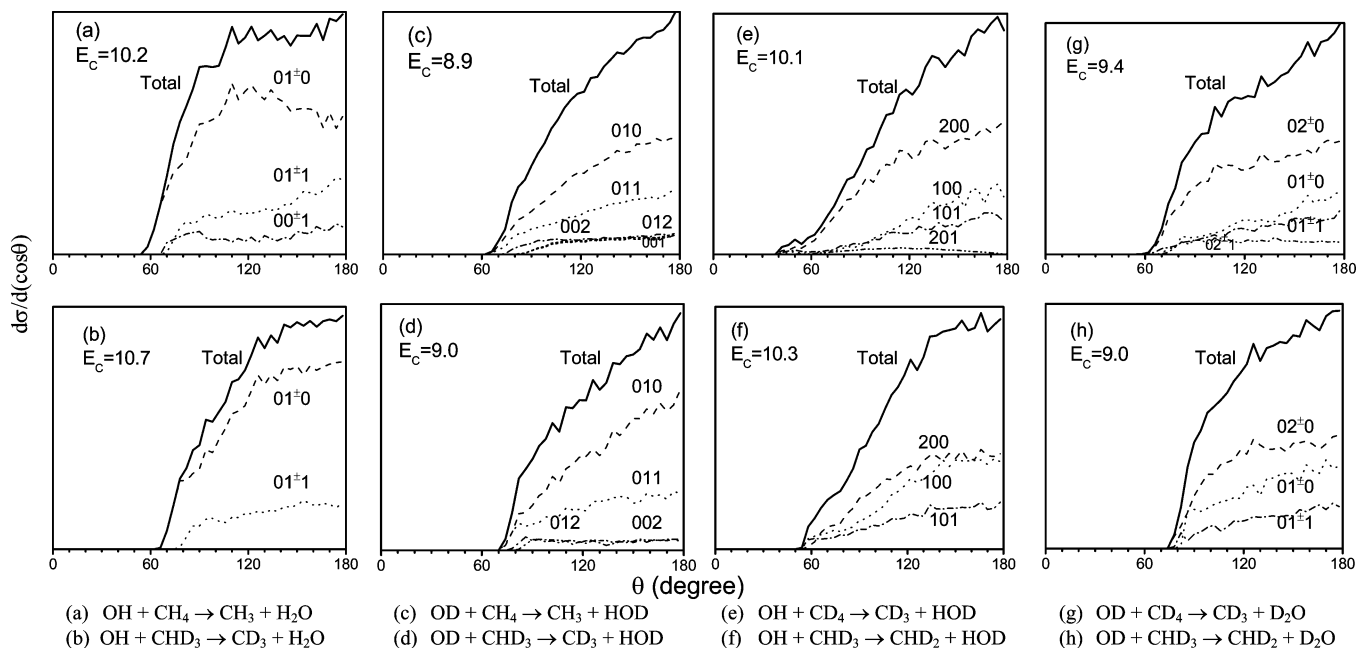


Figure 4. Correlated angular distributions for the raw images shown in Figure 1 are exemplified. Note the striking similarity among them, indicating that both primary and secondary isotope substitutions have little impact to this dynamical attribute.

Comparing the results of reactions a and c and reactions b and d from Figure 3 reveals that in place of OH by OD results in higher branching into the combination/bending excitations. And this effect is more pronounced for the H atom than the D atom transfer reactions (see reactions e vs g and f vs h).

In addition, from Table 1 the deuterated hydroxyl reagent gives rise to somewhat higher rotational excitation of water products. Intuitively, this observation seems consistent with an impulsive bond-breaking mechanism based on the *ab initio* calculated saddle-point geometry and the eigenvector of the imaginary frequency.^{13,26} At the transition state, the transferred H (or D) atom lies close to collinear between the C and O atoms. The hydroxyl O–H bond is almost perpendicular to the C–O axis. The transition state eigenvector corresponding to the imaginary frequency is primarily a motion of the hydrogen atom transferring between the C and O atoms. The replacement of OH by OD shifts the center-of-mass of the hydroxyl moiety more away from the O atom. An impulsive release of the abstracted atom from the above configuration could then exert more torque to the water product, thus inducing a higher rotational excitation.

We now turn our attention to the other secondary isotope effect arising from the deuteration of the H atoms that are not being abstracted from methane. Hence, we shall compare, in Figure 3, the results of the upper and lower panels of each column. Inspections indicated that the more H atoms are in the nonreactive methyl moiety, the larger spread is the water product vibration distribution; see Figure 3a–d. And this spread is the result of a higher probability of bending excitation, as well as a more relaxed distribution in stretching mode. For parts e–h, although a slightly more relaxed stretching excitation is also observed for the CHD_2 product than CD_3 , the combination mode prevails for the latter yielding a somewhat broader distribution. These subtle effects also manifest themselves in terms of the excitation probability and the fractional energy disposal into three different types of vibrational motion of water coproducts (Table 1). The most obvious effects are the less stretching and the more bending excitation for reactions a and c than reactions b and d, respectively. For the other isotopic reactions, i.e., the

D atom transfer cases, the difference is too minor to be concerned.

(C) Pair-Correlated Angular Distributions. Figure 4 summarizes the correlated angular distributions. The general behaviors for various isotopic reactions are quite similar: predominantly backscattered with a cutoff near $60\text{--}70^\circ$ against forward scatterings. This holds true for both primary and secondary isotope substitutions. The only subtle difference is that the reactions forming H_2O or D_2O product display a slightly broader angular distribution than those producing HOD. For a given reaction, the individual state-pair distribution does not vary much from one another. The observation of a nearly invariant angular distribution upon isotope substitution is perhaps not too surprising. This is a heavy + light-heavy reaction. For a direct reaction mechanism, as evidenced from the results in parts 1 and 2 of this series,^{15,16} the product angular distribution will be mainly governed by the trajectories of the two heavy species.²⁷ The isotopic substitution alters the mass of the colliding pair in a minor manner and thus has little impact on the trajectories.

III. Summary

A total of eight isotopically variant reactions $\text{OH/OD} + \text{CH}_4/\text{CD}_4/\text{CHD}_3$ were investigated under crossed-beam conditions. The resulted water products are highly vibrational-excited, with the newly formed bond containing typically 50–60% of total available energy. When the transferred H atom is substituted by a D atom, a significant change in vibrational motions of water products was observed: more stretching excitation, but less excitation in bending and combination modes. That is the primary isotope effect. The secondary isotope effects, both for substituted hydroxyl or methane (unreactive methyl moiety), are as anticipated minor and manifest themselves in spreading the vibrational distribution. In all cases, the isotope effects on angular distributions are quite subtle.

The dynamic isotope effect reported here complements the previous kinetic isotope effect in the literature. In conjunction with the mode-correlation of product pairs and their translational energy dependencies reported in part 1¹⁶ and part 2 of this

series,¹⁵ respectively, this work represents one of the most thorough dynamic characterizations of a polyatomic reaction.

Acknowledgment. This work was supported by the National Science of Council of Taiwan under NSC93-2113-M-001-041 and NSC 94-2915-I-001-011. B.Z. gratefully acknowledges Academia Sinica for a postdoctoral fellowship.

References and Notes

- (1) Johnston, H. S. *Gas-Phase Reaction Rate Theory*; Ronald Pub.: New York, 1966.
- (2) Wayne, R. P. *Chemistry of Atmospheres*, 2nd ed.; Oxford University Press: Oxford, U.K., 1991.
- (3) Ravishankara, A. R. *Annu. Rev. Phys. Chem.* **1988**, *39*, 367.
- (4) Mroz, E. J. *Chemosphere* **1993**, *26*, 45.
- (5) Gordon, S.; Mulac, W. A. *Int. J. Chem. Kinet.* 1975, Symposium 1, 289.
- (6) DeMore, W. B. *J. Phys. Chem.* **1993**, *97*, 8564.
- (7) Dunlop, J. R.; Tully, F. P. *J. Phys. Chem.* **1993**, *97*, 11148.
- (8) Finlayson-Pitts, B. J.; Ezell, M. J.; Jayaweera, T. M.; Berko, H. N.; Lai, C. C. *Geophys. Res. Lett.* **1992**, *19*, 1371.
- (9) Mellouki, A.; Teton, S.; Laverdet, G.; Quilgars, A.; LeBras, G. *J. Chem. Phys.* **1994**, *91*, 473.
- (10) Sharkey, P.; Smith, I. W. M. *J. Chem. Soc., Faraday Trans.* **1993**, *84*, 631.
- (11) Melissas, T.; Truhlar, D. G. *J. Chem. Phys.* **1993**, *99*, 1013.
- (12) Gierczak, V. S.; Talukdar, R. K.; Herndon, S. C.; Vaghjiani, G. L.; Ravishankara, A. R. *J. Phys. Chem. A* **1997**, *101*, 3125.
- (13) Masgrau, L.; Gonzalez-Lafont, A.; Lluch, J. M. *J. Chem. Phys.* **2001**, *114*, 2154; *Theor. Chem. Acc.* **2002**, *108*, 38.
- (14) Espinosa-Garcia, J.; Corchado, J. C. *J. Chem. Phys.* **2000**, *112*, 5731.
- (15) Zhang, B.; Shiu, W.; Liu, K. *J. Phys. Chem. A* **2005**, *109*, 8983.
- (16) Zhang, B.; Shiu, W.; Lin, J. J.; Liu, K. *J. Chem. Phys.* **2005**, *122*, 131102.
- (17) Lin, J. J.; Zhou, J.; Shiu, W.; Liu, K. *Rev. Sci. Instrum.* **2003**, *74*, 2495; *Science* **2003**, *300*, 966.
- (18) Strazisar, B. R.; Lin, C.; Davis, H. F. *Science* **2000**, *290*, 958.
- (19) Zhang, D. H.; Collins, M. A.; Lee, S.-Y. *Science* **2000**, *290*, 961.
- (20) Castillo, J. F. *Chem. Phys. Chem.* **2002**, *3*, 320 and references therein.
- (21) Child, M. S.; Haloner, L. *Adv. Chem. Phys.* **1984**, *57*, 1 and references therein.
- (22) Yu, H.-G. *J. Chem. Phys.* **2001**, *114*, 2967.
- (23) Nyman, G.; Clary, D. C. *J. Chem. Phys.* **1994**, *101*, 5756.
- (24) Nyman, G. *Chem. Phys. Lett.* **1995**, *240*, 571.
- (25) Nyman, G.; Clary, D. C.; Levine, R. D. *Chem. Phys.* **1995**, *191*, 223.
- (26) Bravo-Perez, G.; Alvarez-Idaboy, J. R.; Jimenez, A. G.; Cruz-Torres, A. *Chem. Phys.* **2005**, *310*, 213.
- (27) Zhou, J.; Lin, J. J.; Shiu, W.; Liu, K. *J. Chem. Phys.* **2003**, *119*, 4997.